1300–1308 *Nucleic Acids Research, 2008, Vol. 36, No. 4* *Published online 9 January 2008*
doi:10.1093/nar/gkm1157

Inhibition of DNA replication fork progression and mutagenic potential of 1, N^6-ethenoadenine and 8-oxoguanine in human cell extracts

Joel H. Tolentino[1], Tom J. Burke[2], Suparna Mukhopadhyay[2], W. Glenn McGregor[2,*] and Ashis K. Basu[1]

[1]Department of Chemistry, University of Connecticut, Storrs CT 06269 and [2]Department of Pharmacology and Toxicology, University of Louisville, Louisville KY 40202, USA

Received August 24, 2007; Revised November 11, 2007; Accepted December 14, 2007

ABSTRACT

Comparative mutagenesis of 1,N^6-ethenoadenine (εA) and 8-oxoguanine (8-oxoG), two endogenous DNA lesions that are also formed by exogenous DNA damaging agents, have been evaluated in HeLa and xeroderma pigmentosum variant (XPV) cell extracts. Two-dimensional gel electrophoresis of the duplex M13mp2SV vector containing these lesions established that there was significant inhibition of replication fork movement past εA, whereas 8-oxoG caused only minor stalling of fork progression. In extracts of HeLa cells, εA was weakly mutagenic inducing all three base substitutions in approximately equal frequency, whereas 8-oxoG was 10-fold more mutagenic inducing primarily G→T transversions. These data suggest that 8-oxoG is a miscoding lesion that presents a minimal, if any, block to DNA replication in human cells. We hypothesized that bypass of εA proceeded principally by an error-free mechanism in which the undamaged strand was used as a template, since this lesion strongly blocked fork progression. To examine this, we determined the sequence of replication products derived from templates in which a G was placed across from the εA. Consistent with our hypothesis, 93% of the progeny were derived from replication of the undamaged strand. When translesion synthesis occurred, εA→T mutations increased 3-fold in products derived from the mismatched εA: G construct compared with those derived from the εA: T construct. More efficient repair of εA in the εA: T construct may have been responsible for lower mutation frequency. Primer extension studies with purified pol η have shown that this polymerase is highly error-prone when bypassing εA. To examine if pol η is the primary mutagenic translesion polymerase in human cells, we determined the lesion bypass characteristics of extracts derived from XPV cells, which lack this polymerase. The εA: T construct induced εA→G and εA→C mutant frequencies that were approximately the same as those observed using the HeLa extracts. However, εA→T events were increased 5-fold relative to HeLa extracts. These data support a model in which pol η-mediated translesion synthesis past this adduct is error-free in the context of semiconservative replication in the presence of fidelity factors such as PCNA.

INTRODUCTION

1,N^6-Ethenoadenine (εA) and 8-oxoguanine (8-oxoG) are DNA lesions induced both by endogenous and exogenous agents. εA is formed by a metabolite of the human carcinogen vinyl chloride and various other vinyl compounds (1). It is also formed by lipid peroxidation, which generates several α, β-unsaturated carbonyl compounds (2,3). The level of εA detected in human liver is usually low (~20 lesions per 10^9 dA) (4), but it increases significantly as a result of enhanced lipid peroxidation in patients with genetic metal storage disorders such as Wilson's disease and primary hemochromatosis (5). Diet also influences the level of εA. The mean level of εA is 40-times higher in women who consume diets high in linoleic acid compared with those on high oleic acid diets (6).

*To whom correspondence should be addressed. Tel: 502 852 2564; Fax: 502 852 2492; Email: wgmcgregor@louisville.edu
Correspondence may also be addressed to Ashis K. Basu. Tel: 860 486 3965; Fax: 860 486 2981; Email: ashis.basu@uconn.edu

The authors wish it to be known that, in their opinion, the first two authors should be regarded as joint First Authors.

The exocyclic ring of εA blocks the Watson–Crick base pairing region, but *syn* rotation of the base allows Hoogsteen-type base pairing (7,8). Early studies on *in vitro* translesion synthesis across εA indicated that misincorporation may depend on the DNA polymerase used (9,10) and that G incorporation opposite εA occurs more frequently. More recent studies with the Y family polymerases showed that translesion synthesis past εA is 100-fold more efficient with human pol η compared to pol κ, although significant base substitutions and one-base deletions occurred with each of these two polymerases (11). Misincorporation of all three nucleotides was also observed in cells. However, εA is only weakly mutagenic in *Escherichia coli* (12,13). In contrast, in single-stranded (ss) DNA, εA is highly mutagenic in simian kidney cells, inducing primarily εA→G transitions (13). Analysis of the sequence of duplex plasmids with a single lesion replicated in human cells indicates that only about 10% of the progeny reflected replication using the strand that contained the εA. In these cases, replication proceeds by translesion synthesis (TLS) mechanisms, which is predominantly error-free; however, all three nucleotide changes have also been detected in 7–14% of the TLS progeny (14). In most cases, replication proceeds using the undamaged strand as the template, suggesting that εA is a block to DNA replication (14). εA is a substrate for alkylpurine DNA-*N* glycosylase, and homologs of this enzyme have been found in *E. coli*, *Saccharomyces cerevisiae*, rat and human cells (15,16).

8-OxoG is a ubiquitous oxidative lesion in DNA formed by exogenous agents such as ionizing radiation (17). It is also formed during endogenous metabolic processes (18). Mutagenicity of 8-oxo-dG determined in a number of studies in *E. coli* and in mammalian cells showed that it predominantly induces G→T transversions (19–21). The mutation frequency (MF) of a single 8-oxo-dG is in the range of 3–8% in ss DNA in both bacterial and mammalian cells (reviewed in 22), though higher MF in a specific sequence was noted (23). In double-stranded (ds) DNA the MF is much lower (24), presumably due to a more efficient repair. Multiple repair systems have evolved to repair this damage (see 25,26 for reviews). 8-Oxoguanine DNA glycosylase, the product of *mutM*, also known as Fpg protein, in bacteria and its eukaryotic functional homolog, the Ogg1 protein, efficiently repairs 8-oxoG opposite cytosine. For 8-oxoG: A pairs, the MYH (MUTYH), a mammalian homolog of bacterial MutY protein, acts as the adenine DNA glycosylase (27). The importance of oxidative damage repair was underscored in a study (28), which demonstrated that inherited variants of the human homolog of *mutY*, *MYH*, is associated with somatic G: C→T: A mutations in colorectal cancer.

Irrespective of how mutagenic a lesion might be in ss DNA, because of a more efficient repair, mutagenicity of the lesion is drastically reduced in duplex DNA. In addition, stalling (or blockage) of replication at the lesion site often result in a strand-bias of replication, such that a major fraction of the progeny arises from the undamaged strand. We wished to evaluate the mutational types and frequencies of these two important lesions in extracts of human cells without any strand maker such as a mismatch or reporter sequence, which might trigger some unusual biological response. Since translesion synthesis across these two lesions by pol η has been reported (11,29), we also compared the mutagenicity of εA and 8-oxoG in extracts of xeroderma pigmentosum variant (XPV) cells, which are defective in this DNA polymerase.

MATERIALS AND METHODS

Materials

[γ-^{32}P]ATP was from Du Pont New England Nuclear (Boston, MA, USA). T4 DNA ligase and T4 polynucleotide kinase were obtained from New England Bioloabs (Beverly, MA, USA). The replication template M13mp2-SV*ori*L, *E. coli* strains NR9162 (*mutS*), CSH50 and NR9099 were gifts from Dr Thomas Kunkel, National Institute of Environmental Health Sciences, NIH.

Methods

Synthesis and characterization of oligonucleotides. The 26 mer oligonucleotides, 5′CGG CCA GTG CC(εA) TCG CTA CCA ATT CG-3′, 5′-CGG CCA GTG CCA TCG$^{8\text{-oxo}}$ CTA CCA ATT CG-3′,were synthesized by the Midland Certified Reagent Company, Inc (Midland, TX, USA). The deprotection of εA 26-mer was carried out in the presence of 1,8-diazabicyclo[5.4.0]undec-7-ene as described (30). The 8-oxoG oligonucleotide was deprotected with concentrated NH_4OH for 18 h at 55°C in the presence of 0.25 M β-mercaptoethanol. The oligonucleotides were purified by HPLC followed by denaturing polyacrylamide gel electrophoresis. Mass spectrometric analysis by MALDI-TOF verified the molecular weight of the oligonucleotides.

Construction of M13 vectors containing a single εA or 8-oxoG. The 26 mer oligonucleotide (48 pmol) containing the lesion was phosphorylated using 1.5 U of T4 polynucleotide kinase (10 U/μl) and 0.5 μl of 10 mM ATP in 70 mM Tris–HCl, 10 mM $MgCl_2$, 5 mM dithiothreitol, pH = 7.6 at 37°C for 30 min. The enzyme was inactivated at 65°C for 20 min. The phosphorylated primer was annealed to the ss M13mp2SV DNA template (6 pmol) in 20 mM Tris–HCl, pH = 7.4, 2 mM $MgCl_2$, 50 mM NaCl by heating at 70°C for 5 min, followed by cooling down to room temperature over a period of 2 h. The annealed primer was extended by adding 45 U of T4 DNA polymerase (3 U/μl) and 2 μl 50% glycerol in 20 mM Tris-HCl, pH = 7.4, 2 mM dithiothreitol, 10 mM $MgCl_2$, 0.5 mM dNTP's and 0.4 mM ATP at the following conditions: incubation in ice for 10 min, room temperature for 5 min and at 37°C for 1.5 h. The nick on the newly synthesized strand was ligated using 400 U of T4 DNA Ligase (400 U/μl) at 15°C overnight. Following inactivation of the enzymes at 65°C for 20 min, methylation of the newly synthesized strand was carried out by adding 32 U of *dam* Methylase (8 U/μl) and 0.8 μl of 32 mM *S*-adenosylmethionine in 50 mM Tris–HCl, 10 mM EDTA, 5 mM 2-mercaptoethanol, pH = 7.5 at 37°C for 1 h. The verification of successful methylation was performed by treating 1 μg of each construct with 1 U

*Dpn*I (20 U/μl) in 50 mM potassium acetate, 20 mM Tris–acetate, 10 mM magnesium acetate, 1 mM dithiothreitol, pH = 7.9 at 37°C for 1 h. Samples (0.5 μg each) of the ss DNA template, ds M13mp2SV40, unmethylated construct, methylated construct, *Dpn*I-treated unmethylated and methylated constructs are run in 0.8% agarose gel in 1× TAE Buffer for 2.5 h at 4°C. Replicative form I (RF I) DNA was obtained by purification on two CsCl gradients according to published procedures (31,32).

Cell lines, culture conditions and preparation of cell extracts. Skin fibroblasts derived from xeroderma pigmentosum variant patient XP115Lo were immortalized with hTERT and were obtained from Dr Lisa McDaniels (University of Texas Southwestern Medical School, Dallas, TX, USA) under the terms of MTA 3025 between WGM and Geron Corporation. Cells were cultured under standard conditions in DMEM, 10%FCS and antibiotics. HeLa cells were cultured under the same conditions, in DMEM supplemented with 10% SCS and antibiotics. Replication-competent cell extracts were prepared by hypotonic nuclear extraction according to the method of Li and Kelly (33), as described (31,32).

Two-dimensional (2D) gel electrophoresis. Replication fork movement past the lesion site was determined by a modification of the method of Brewer and Fangman (34,35). Replication reactions were performed as described but stopped after 30 min. The products were purified and digested with the indicated restriction enzyme(s). Electrophoresis in the first dimension was carried out at 0.4 V/cm for 68 h in 0.4% agarose gels containing 0.2 μg/ml ethidium bromide, prepared with TBE buffer. The lanes were excised and cast into a second gel that was 1% agarose in TBE buffer containing 0.2 μg/ml ethidium bromide. The second dimension was carried out at 90° with respect to the first, and electrophoresis continued at 1.5 V/cm for 24 h. The gels were dried and exposed to phosphor screens and scanned with a Typhoon PhosphorImager.

Analysis of the scanned images was carried out using the polygon tool and ImageQuant. Only replication-intermediate arcs were quantified, using volume integration with no background subtraction. The intensity of bubble and fork arcs were expressed as percentages of the sum of all replicating structures detected.

Replication and analyses. Reactions, carried out as described previously (31), contained 40 ng of the template in a total volume of 25 μl. T antigen was omitted from the control reaction tubes. Following addition of replication-competent cell extract (75–100 μg of protein), the reaction mixtures were incubated for 1 h at 37°C. An aliquot (1/10 volume) was taken for determination of [α-^{32}P]dCTP incorporation into acid-insoluble material. An internal standard consisting of pUC19 restricted with *Hin*dIII and end-labeled with ^{32}P was added to each sample. The DNA was extracted and treated with *Dpn*I to digest any fully methylated (i.e. unreplicated) templates. Aliquots of the samples were electrophoresed on 1% agarose gels containing 0.5 μg/ml ethidium bromide. The density of the bands corresponding to covalently closed circular (form I) DNA was quantified by use of ImageQuant software in a Molecular Dynamics PhosphorImager. The amount of form I synthesis as a percentage of synthesis of DNA from the control (undamaged) template was corrected for loss of the DNA during the purification procedure by normalizing the density of the form I band to that of the internal control.

An aliquot of the purified, newly replicated DNA was electroporated into *E. coli* strain NR9162, which is deficient in mismatch repair (*mutS*) to avoid correction of heteroduplex DNA. Immediately after electroporation, these bacteria were coplated with an indicator strain, *E. coli* CSH50. The transfected bacteria replicate the bacteriophage and infect the surrounding indicator bacteria, resulting in colorless plaques in the lawn of indicator bacteria. The assay scores only newly replicated, covalently closed circular DNA molecules. After overnight incubation at 37°C, the plates were overlaid with nylon membranes (Boehringer Mannheim) and the plaques were screened for mutations in the region of the lesion by hybridization. Since the MF for εA was low, we used both mutant probe and wild-type probe to detect mutations, and all putative mutants were sequenced. For 8-oxoG, preliminary analysis showed that only 8-oxoG→T mutations occurred at a significant level. The only other type of mutant detected was 8-oxoG→C, which occurred at level of 5–10% of the G→T events. We therefore concentrated in determining only the 8-oxoG→T mutations.

RESULTS AND DISCUSSION

Construction of M13mp2SVoriL vectors

The template was derived from M13mp2S*Ori*L (36), which contains the SV40 origin of replication and will undergo semiconservative bidirectional replication in the presence of SV40 large T antigen and replication-competent extracts derived from human cells. A +11 mutant clone of M13mp2S*Ori*L was generated by inserting d(GGTAGCGATGG) into the *Eco*RI site of the multiple cloning region of the bacteriophage (Figure 1) (32). As shown in Scheme 1, an unmodified or modified 5′-phosphorylated 26 mer oligonucleotide was annealed to the ss M13 DNA, and the primer was extended with T4 DNA polymerase and deoxynucleotide triphosphates. Ligation was carried out with T4 DNA ligase and the duplex DNA was methylated with *dam* methylase. Progress in each step was analyzed by agarose gel electrophoresis. Figure 2 shows the ss M13 DNA (lane 1) on which the εA 26-mer was annealed. Lanes 3 and 4 show the extended and ligated DNA before and after methylation, respectively. Lane 5 shows the DpnI-digested construct, which completely eliminated the faster running form I DNA. The form I DNA was purified by cesium chloride density gradient centrifugation in the presence of ethidium bromide. The latter was removed by ion-exchange chromatography, phenol-chloroform extraction and ethanol precipitation. The final yield of covalently closed circular (form I) DNA was 8–10%.

Results from the 8-oxoG, unmodified constructs, and the mismatched constructs were also similar (data not shown).

Replication fork movement past the lesion site

To determine the extent of replication fork blockage by εA or 8-oxoG, we examined the topology of DNA replication intermediates by 2D gel electrophoresis. This technique has proven to be useful for characterizing origins of replication (34,35). The properties of bubble arcs and single fork arcs in such gels have been characterized (37,38), and the technique has provided insights into replication fork bypass of a T–T cyclobutane pyrimidine dimer in the leading strand template (39).

The progression of the replication fork up to and beyond the lesion was examined by digesting the replicated molecules with *Cla*I, which cuts M13mp2 + 11 ~ 760 bases to the right of either adduct and ~180° away from the SV40*ori* (Figure 1). This results in two linear fragments of 4.3 and 3.1 kb. The larger fragment contains the SV40*ori* located asymmetrically (Figure 3A), and 2D gel electrophoresis of replicated undamaged templates revealed two families of DNA replication intermediates associated with the 4.3 kb fragment with different topologies (Figure 3A and B). These include structures with a bubble arc and those with a single fork arc. The bubble arc structures represent intermediates that have not yet progressed beyond the *Cla*I site closest to the ori, and single forks result when replication has proceeded beyond this site. Such progression resulted in the appearance of single fork arcs associated with the 3.1 kb fragment. Analysis of the replication intermediates derived from templates containing εA (Figure 3C) or 8-oxoG (Figure 3D) clearly show that single fork arcs are associated with the 4.3 kb fragment. This implies that the right fork has passed the *Cla*I site at position 7043 and can therefore be inferred to have bypassed the lesion in the leading strand template. Although it is formally possible that the right fork is completely blocked and the left fork proceeds all the way around to replicate past both restriction sites, previous studies have shown that this does not happen during the short incubation times used in these experiments (39). Examination of the gels indicates replication intermediates that correspond to the 7.4 kb template, indicated by the open triangles in Figure 3B–D.

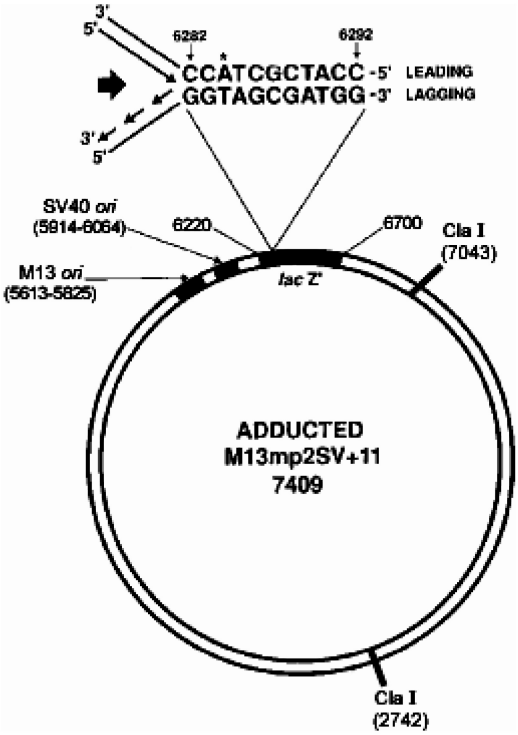

Figure 1. Construction of M13mp2-SV +11 with a single ethenoadenine or 8-oxoguanine adduct. The ethenoadenine was placed in position 6284, indicated by A* in the diagram. The 8-oxoguanine was placed in position 6287, but is not indicated in the diagram for clarity. Semiconservative bidirectional replication proceeds from the center of the SV40 *ori*, such that the right fork traverses only ~300 bases before it encounters the lesion. Therefore, the lesions are presumed to be in the leading strand template. Control templates did not contain DNA damage, and mismatched templates contained a guanine residue opposite the lesion. The *Cla*I restriction sites used in the 2D gel electrophoresis analysis of the replication products are also indicated.

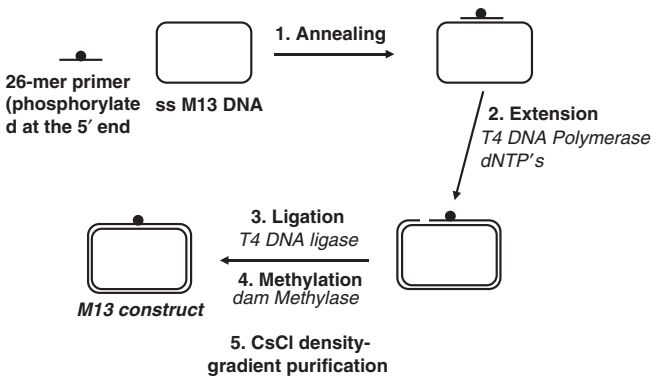

Scheme 1. General protocol for making the M13mp2SV*ori*L +11 construct.

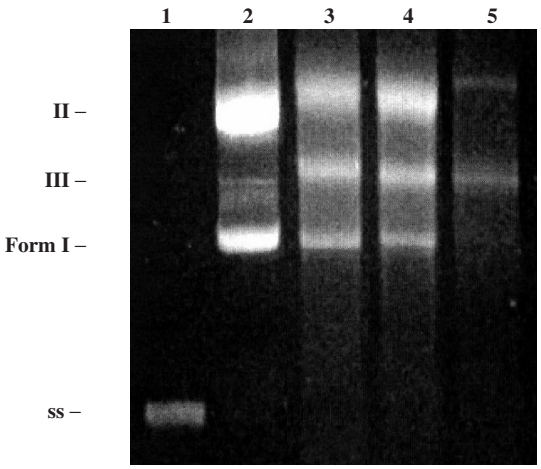

Figure 2. Agarose gel electrophoresis of M13mp2SV*ori*L +11 construct containing εA. Lane 1: ss M13mp2SV; Lane 2: ds M13mp2SV standard; Lanes 3 and 4, respectively, represent the εA construct following primer extension (and ligation) before and after treatment with *dam* methylase; Lane 5 shows the material from lane 4 after *Dpn*I digestion.

These products are indeed replication intermediates since they have incorporated the radioactive dCTP precursor and do not appear if T-antigen is omitted from the reaction (data not shown). These large structures have been interpreted to be replication intermediates in which the right fork has been stalled by the lesion in the leading strand template, but downstream priming on the lagging strand template continues for some distance. This 'fork uncoupling' results in a single-strand region in the leading strand template, which is not subject to cutting by *Cla*I. This interpretation was originally proposed by Cordiero-Stone and colleagues (39) to explain similar structures observed when a T–T cyclobutane pyrimidine dimer was placed in the leading strand template. As diagrammed in Figure 4, A represents initiation of replication around the SV40 *ori* and B, fork progression in templates that do not contain a lesion. Coordinate leading and lagging strand synthesis continues past the *Cla*I site and the resulting double-strand regions are subject to cutting by the restriction enzyme. In the case of a replication-blocking lesion in the leading strand template (Figure 4C and D), synthesis of the nascent strand using that template is blocked. However, replication using the lagging strand template may continue downstream for some distance. This results in a population of large intermediates that are not cut by the enzyme. The magnitude of this arc relative to the other replication intermediates is a measure of the degree of inhibition of fork progression. This high molecular weight intermediate is clearly most pronounced when the template containing the εA is replicated (Figure 3C), indicating that this lesion blocks replication to a greater extent than the 8-oxoG (Figure 3D). Quantitation of the relative intensities of these arcs indicates that 8-oxoG increases the intensity of this arc 1.6-fold over the control template, compared with 6-fold for εA. These results support the conclusion that εA in the leading strand template represents a significant block

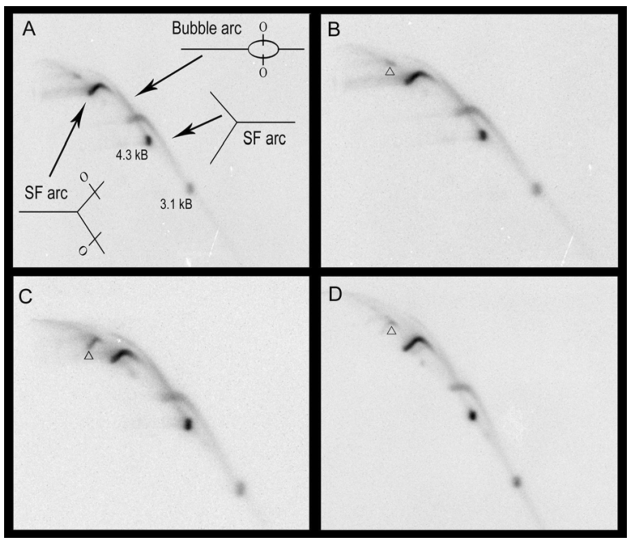

Figure 3. 2D gel electrophoresis of replication intermediates digested with *Cla*I. Extracts from HeLa cells were incubated for 30 min in the presence of T-antigen with control DNA (**A** and **B**) or DNA containing a single ethenoadenine (**C**) or 8-oxoguanine (**D**), as described in Materials and Methods section. The purified DNA was digested with *Cla*I and separated by 2D gel electrophoresis. The positions of the linear 4.3 and 3.1 kb fragments are indicated in panel A, together with the replication intermediates associated with these fragments. SF arc means single fork arc, whereas bubble arc indicates the replication forks that had not yet reached the *Cla*I sites. The arcs indicated by the open triangles in panels B, C and D are discussed in the text.

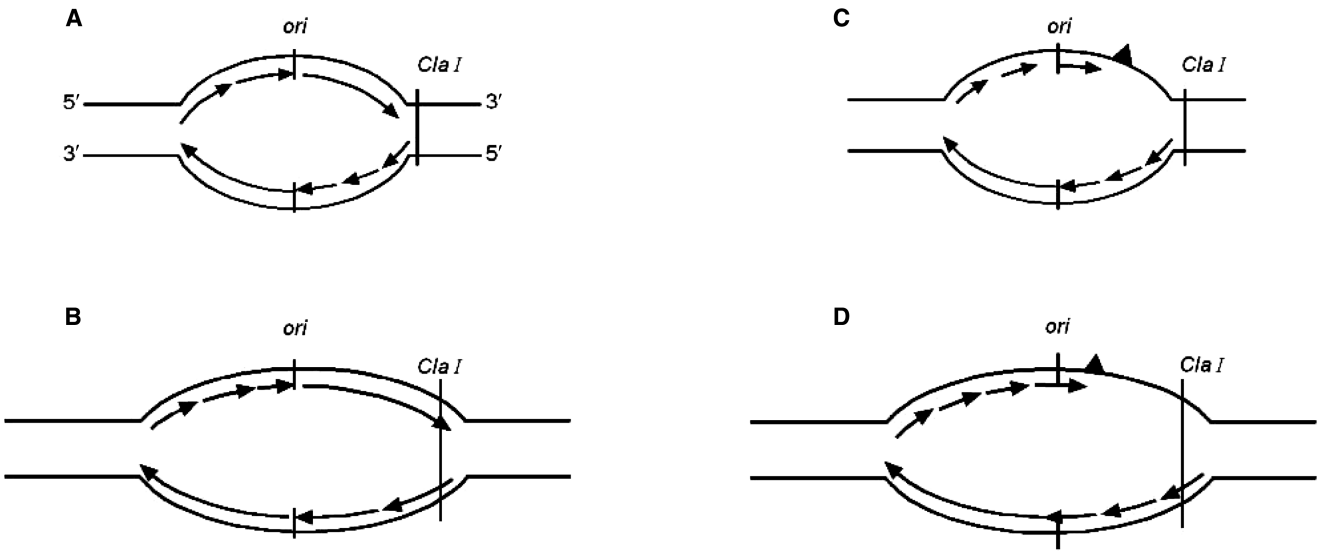

Figure 4. Proposed replication intermediates. The template used in these studies is a 7.4 kbp plasmid that contains the SV40 origin of replication (*ori*). The helicase activity of large T antigen allows assembly of DNA replication forks and subsequent bidirectional replication that proceeds from the *ori*. Panels (**A**) and (**B**) represent initiation and progression of fork movement when there is no impediment to fork progression. The two *Cla*I sites (shown in Figure 1) remain principally in double-stranded regions. Most of the replication intermediates are cut by the restriction enzyme, such that there is very little of the full-length intermediate denoted by the open triangles in Figure 3B and D. Panels (**C**) and (**D**) illustrate blockage of the right leading strand replication complex by εA with progression of replication of the lagging strand (fork uncoupling). Replication of the lagging strand has been estimated to proceed for ~700 bases in this system when the leading strand is blocked by a lesion in that template (39). The resulting single-stranded region is not cut by *Cla*I, and this is reflected by an increased intensity in the large intermediate denoted by the open triangle in Figure 3C.

Table 1. Mutagenicity of εA and 8-oxoG in extracts of HeLa and XPV cells

Cell nine	Lesion	Total plaques analyzed	Type of Mutation			Mutation frequency ($\times 10^{-4}$)
			→C	→G	→T	
HeLa	εA	12 782	2	–	–	1.6
	εA	10 486	–	–	3	2.9
	εA	15 351	–	3	–	2.0
	$G^{8\text{-oxo}}$ (un)	19 551	ND	ND	180	92
	$G^{8\text{-oxo}}$	14 606	ND	ND	101	69
XPV	εA	13 158	2	–	–	1.5
	εA	12 475	–	–	18	14.4
	εA	17 749	–	2	–	1.1
	$G^{8\text{-oxo}}$ (un)	17 039	ND	ND	149	88
	$G^{8\text{-oxo}}$	18 922	ND	ND	106	56

ND, not determined; $G^{8\text{-oxo}}$ (un) indicates construct that was not methylated with *dam* methylase.

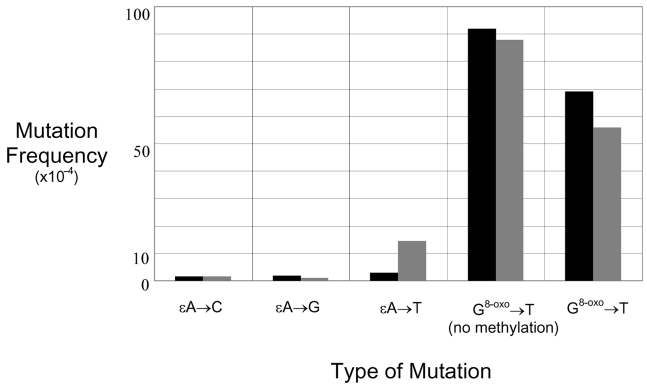

Figure 5. Mutational frequency ($\times 10^{-4}$) of εA and 8-oxoG in HeLa (dark bars) and XPV (gray bars) extracts.

to fork progression, while 8-oxoG constitutes only a minor impediment.

Mutagenicity of εA and 8-oxoG in extracts of human cells

As expected, in the absence of a strand-marker most of the progeny from the adducted vector contained no mutations. In order to collect all possible mutational events, we screened the progeny derived from the εA template with all possible base pair mutant probes and the non-mutant or wild-type probe. Our analysis using a combination of oligonucleotide hybridization and DNA sequencing indicated that small frameshifts (additions or deletions) did not occur during replication of any of these constructs. For εA all three base substitutions occurred with approximately equal frequency in HeLa cells, but the level of mutagenesis was low (total MF $\sim 7 \times 10^{-4}$) (Table 1). In contrast, 8-oxoG, however, induced G→T transversions at a 10-fold higher level (MF 69×10^{-4}) (Table 1 and Figure 5). We hypothesized that the low frequency of mutations induced by εA is a reflection of the strong block to replication that this adduct presents. In this case, replication can be completed by error-free template switching mechanisms or potentially error-prone translesion synthesis. To examine this, we assessed the fraction of progeny derived from these to two mechanisms using a strand marker. We made two constructs in which εA or A in the (−) strand was placed opposite G in the (+) strand. Approximately 60% progeny derived from the unmodified A:G mismatched construct contained a G in the (+) strand (Table 2). In contrast, ∼93% progeny in the εA:G construct contained a G in the (+) strand (Table 2). This is consistent with εA being a strong block of replication, with replication proceeding by copying the information in the undamaged strand (i.e. template switching). In the mismatched construct, it is noteworthy that the εA→T mutations increased 3-fold to 10×10^{-4} (Table 2), in comparison to the εA: T construct that produced 3×10^{-4} εA→T. If ∼7% progeny came from the εA-containing strand, the calculated εA→T mutations derived from the lesion containing strand of the εA: T and εA: G construct, respectively, were 0.4 and 1.4%, which reflects a low error rate during translesion synthesis and/or efficient repair. One explanation for the 3-fold increased mutagenesis from the mismatched construct is a less efficient repair in the εA: G construct. Similar experiments with 8-oxoG mismatched with G showed that compared with 54% from the control G: G construct, 70% progeny from the 8-oxoG: G construct contained a G in the (+) strand (Table 3). Therefore, 30% progeny was derived from TLS of 8-oxoG in the (−) strand relative to 46% in the control, which suggests that 8-oxoG stalled but did not provide a major block of replication as we noted in our fork progression study. It is noteworthy that the 8-oxoG→T transversions increased nearly 7-fold to 4.8% (Table 3). Therefore, we conclude that 8-oxoG repair in 8-oxoG: G mismatch, similar to εA: G, is inefficient in HeLa extract.

It is important to consider if abasic sites formed by excision of the lesions by a glycosylase were responsible for the mutations observed in our study. We believe it unlikely because earlier studies have shown that most (∼85%) TLS events involve insertion of dAMP opposite a synthetic abasic site in several human cell lines (40), whereas we noted a very different signature of εA-induced mutations in this study. Evidently, this argument cannot be used for 8-oxoG because dAMP insertion is the predominant misincorporation event opposite both 8-oxoG and abasic site. However, in an *in vitro* study it was shown that in HeLa cell extracts εA is repaired

Table 2. Replication of εA:G and A:G constructs in extracts of HeLa cells[a]

M13 construct	Progeny containing a G	Progeny containing a T (arising from the A-containing (−) strand)	εA→T mutants
A : G	1353 of 2232 (61%)	991 of 2323 (43%)	N/A
εA : G	1710 of 1836 (93%)	188 of 2052 (9%)	16 of 15965 (0.1% overall but 1.4% from εA strand)[b]

[a]The constructs contained a G in the (+) strand and an εA or A opposite it in the (−) strand.
[b]The percent εA→T from εA strand was calculated on the basis of 7% (or 1118) plaques arising from the strand containing εA.

Table 3. Replication of 8-oxoG : G and G : G constructs in extracts of HeLa cells[a]

M13 construct	Progeny containing a G	8-oxoG→T mutants
G : G	708 of 1321 (54%)	N/A
8-oxoG : G	1291 of 1840 (70%)	455 of 9501 (4.8% overall but 16.0% from 8-oxoG strand)[b]

[a]The constructs contained a G in the (+) strand and an 8-oxoG or G opposite it in the (−) strand.
[b]The percent 8-oxoG→T from 8-oxoG strand was calculated on the basis of 30% (or 2850) plaques arising from the strand containing 8-oxoG.

by both short and long patch repair, whereas 8-oxoG is repaired mainly by the short patch pathway (41). This investigation also demonstrated that the repair kinetics of 8-oxoG is much slower than that of a preformed abasic site, which also suggests that the 8-oxoG→T mutations in our study were unlikely to be derived from abasic sites.

In a prior study, Moriya and coworkers found εA to be mutagenic in human cells with MF between 7 and 14% in duplex DNA after the progeny from the undamaged strand was eliminated (14). Furthermore, in this study in comparison to 8-oxoG, εA was found to be much more mutagenic (14). Our data is in stark contrast to this study, and we found 8-oxoG to be more mutagenic than εA. We believe that the primary reason for this difference stems from the difference between the two experimental systems. The sequence contexts used in these two studies were different. More importantly, in the Levine *et al.* (14) study εA was incorporated opposite a guanine and the two bases adjacent to the lesion also contained mismatches, which would generate a small bubble. εA opposite guanine rotates to *syn* and this mismatched region might have resulted in a less efficient repair. In contrast, in the M13 vector we used, the lesion was located in a perfectly complementary region opposite thymine, which probably triggered a more efficient repair. We investigated this possibility by incorporating εA opposite G and, consistent with our hypothesis, the εA→T substitutions increased 3-fold. *In vitro* repair studies showed that εA opposite T or C is excised at a comparable rate (42), but the kinetics of repair opposite G or in a mismatched bubble have not been determined.

Published reports of primer extension assays using purified polymerases to synthesize past εA or 8-oxoG adducts in the templates indicate that pol η bypasses 8-oxoG efficiently and accurately (29), whereas it bypasses εA in an error-prone manner (11). If these results reflect the function in pol η *in vivo*, then the absence of this enzyme might result in enhanced mutagenesis of 8-oxoG and reduced mutagenesis of εA. Therefore, we examined mutational consequence of these two lesions in XPV cells, which do not have functional pol η. To our surprise, we found that εA→T mutations increased 5-fold in extracts of XPV cells, whereas the εA→C and εA→G substitutions remained approximately the same. Furthermore, the frequency of 8-oxoG→T mutations was 20% lower (MF 56×10^{-4}) when the modified templates were replicated with extracts from XPV cells relative to those replicated with extracts from HeLa cells. The helix-distorting lesions that block replication fork progression are now known to require the Y family polymerases for TLS. This has been most intensively studied for pol η, and it is generally accepted that a principal role of this polymerase is to synthesize past UV-induced cyclobutane pyrimidine dimers in an error-free manner (43). However, its role, if any, in mutagenic TLS past other damages is much less certain.

Since the frequency of 8-oxoG→T mutations did not change in the absence of pol η, it can be inferred that this enzyme is not principally involved in TLS past such adducts in human cells. It is also possible that another Y-family enzyme with similar bypass characteristics assumes its function. Since these miscoding lesions do not present a significant block to DNA replication, one might speculate that the replication complex synthesizes past them with minimal requirements for Y-family polymerases. In yeast, however, pol η seems to play a critical role in the error-free bypass of 8-oxoG, whereas pol δ stalls at both insertion and extension steps (29). For the mutagenic bypass of 8-oxoG, it was suggested that either pol η or pol ζ can extend from the dAMP incorporated opposite 8-oxoG by pol δ, but pol ζ is likely to be more effective at this step since it is nearly as efficient at extending from the A opposite 8-oxoG as it is in extending C opposite G, whereas pol η extends from an A opposite 8-oxoG with an ~6-fold reduced efficiency (44). Our result in XPV extract suggests that pol ζ might play the role of extender of A opposite 8-oxoG rather than pol η, but another polymerase must have successfully replaced

the role of accurate replication by pol η. Though there is a high degree of evolutionary conservation of the mechanism of TLS in yeast and human cells, whether the human DNA polymerases behave similarly toward 8-oxoG remains to be investigated. It is noteworthy that human polymerase κ also is efficient in extending from the nucleotides incorporated opposite 8-oxoG by pol δ (45). It should be reiterated, however, that despite facile bypass of 8-oxoG by these purified specialized DNA polymerases, their role in a cell is not clear at this time.

In this context, it is intriguing to note that the absence of pol η resulted in a 5-fold *increase* in εA→T substitutions, not a *decrease* as predicted by the primer extension data quoted above. Pol η is known to require PCNA for optimal activity (46,47), and the data in the current study support a role for this enzyme in error-free TLS of εA adducts. In the absence of pol η, another Y-family polymerase presumably assumes its function in a manner analogous to the error-prone TLS activity of pol ι past UV photoproducts (48,49). Although TLS is the source of virtually all mutations induced by replication-blocking lesions, the overwhelmingly preferred mode of resolution of blocked replication forks is recombination. This is supported by the finding in the current study that most progeny phage derived from templates that contained an εA resulted from preferential copying of the undamaged strand. This method of lesion bypass presumably proceeds by fork uncoupling and template-switching mechanisms.

In conclusion, in duplex DNA εA was a strong block to replication fork progression but was weakly mutagenic in HeLa cell extracts, inducing all three base substitutions in approximately equal frequency. In contrast, 8-oxoG presented a weak block to fork progression but was 10-fold more mutagenic inducing primarily G→T transversions. In XPV cells, mutagenicity of 8-oxoG was only slightly lower, while εA→T substitutions increased 5-fold. These data support a model in which the replication-blocking lesion εA requires a Y-family polymerase for TLS, which may be pol η acting in an error-free manner. In contrast, 8-oxoG lesions do not present a significant block to fork progression. Instead, in most cases the replication complex itself correctly interprets the altered base as 'G'. Rarely, mutations may be generated when the lesion is misinterpreted as 'T'. Although data indicate that pol δ is not very efficient in bypassing 8-oxoG, recent evidence implicates pol ε in replication of the leading strand template (50). To our knowledge, the lesion bypass characteristics of this enzyme have not been studied. In either case, our data support a model in which 8-oxoG presents a minimal block to fork progression. In this case, the principal mode of bypass may be the replication fork itself, with the specialized DNA polymerases playing a secondary role.

ACKNOWLEDGEMENTS

National Institute of Environmental Health Sciences (ES09127 and ES013324 to A.K.B.) and National Cancer Institute (CA112167 to W.G.M.). Funding to pay the Open Access publication charges for this article was provided by NIEHS.

Conflict of interest statement. None declared.

REFERENCES

1. Bartsch,H., Barbin,A., Marion,M.J., Nair,J. and Guichard,Y. (1994) Formation, detection, and role in carcinogenesis of ethenobases in DNA. *Drug Metab. Rev.*, **26**, 349–371.
2. Chung,F.L., Chen,H.J. and Nath,R.G. (1996) Lipid peroxidation as a potential endogenous source for the formation of exocyclic DNA adducts. *Carcinogenesis*, **17**, 2105–2111.
3. Bartsch,H. (1999) Keynote address: exocyclic DNA adducts as new risk markers for DNA damage in man. In Singer,B. and Bartsch,H. (eds), *Exocyclic DNA Adducts in Mutagenesis and Carcinogenesis*, IARC Scientific Publ., No 150: Lyon, France, pp. 1–16.
4. Nair,J., Barbin,A., Guichard,Y. and Bartsch,H. (1995) 1,N^6-ethenodeoxyadenosine and 3,N^4-ethenodeoxycytine in liver DNA from humans and untreated rodents detected by immunoaffinity/^{32}P-postlabeling. *Carcinogenesis*, **16**, 613–617.
5. Nair,J., Carmichael,P.L., Fernando,R.C., Phillips,D.H., Strain,A.J. and Bartsch,H. (1998) Lipid peroxidation-induced etheno-DNA adducts in the liver of patients with the genetic metal storage disorders Wilson's disease and primary hemochromatosis. *Cancer Epidemiol. Biomark. Prev.*, **7**, 435–440.
6. Nair,J. (1999) Lipid peroxidation-induced etheno-DNA adducts in humans. In Singer,B. and Bartsch,H. (eds), *Exocyclic DNA Adducts in Mutagenesis and Carcinogenesis*, IARC Scientific Publ., No 150: Lyon, France, pp. 55–62.
7. Kouchakdjian,M., Eisenberg,M., Yarema,K., Basu,A., Essigmann,J. and Patel,D.J. (1991) NMR studies of the exocyclic 1,N^6-ethenodeoxyadenosine adduct (εdA) opposite deoxythymidine in a DNA duplex. Non-planar alignment of dA (*anti*) and dT (*anti*) at lesion site. *Biochemistry*, **30**, 1820–1828.
8. de los Santos,C., Kouchakdjian,M., Yarema,K., Basu,A., Essigmann,J. and Patel,D.J. (1991) NMR studies of the exocyclic 1,N^6-ethenodeoxyadenosine adduct (εdA) opposite deoxyguanosine in a DNA duplex. dA (*syn*): dG (*anti*) pairing at lesion site. *Biochemistry*, **30**, 1828–1835.
9. Barbin,A., Bartsch,H., Leconte,P. and Radman,M. (1981) Studies on the miscoding properties of 1,N^6-ethenoadenine and 3,N^4-ethenocytosine, DNA reaction products of vinyl chloride metabolites, during *in vitro* DNA synthesis. *Nucleic Acids Res.*, **9**, 375–387.
10. Singer,B., Abbott,L.G. and Spengler,S.J. (1984) Assessment of mutagenic efficiency of two carcinogen-modified nucleosides, 1,N^6-ethenodeoxyadenosine and O^4-methyldeoxythymidine, using polymerases of varying fidelity. *Carcinogenesis*, **5**, 1165–1171.
11. Levine,R.L., Miller,H., Grollman,A.P., Ohashi,E., Ohmori,H., Masutani,C., Hanaoka,F. and Moriya,M. (2001) Translesion DNA synthesis catalyzed by human pol η and pol κ across 1,N^6-ethenodeoxyadenosine. *J. Biol. Chem.*, **276**, 18717–18721.
12. Basu,A.K., Wood,M.L., Niedernhofer,L.J., Ramos,L.A. and Essigmann,J.M. (1993) Mutagenic and genotoxic effects of three vinyl chloride-induced DNA lesions: 1,N^6-ethenoadenine, 3,N^4-ethenocytosine, and 4-amino-5-(imidazol-2-yl)imidazole. *Biochemistry*, **32**, 12793–12801.
13. Pandya,G.A. and Moriya,M. (1996) 1,N^6-ethenodeoxyadenosine, a DNA adduct highly mutagenic in mammalian cells. *Biochemistry*, **35**, 11487–11492.
14. Levine,R.L., Yang,I.-Y., Hossain,M., Pandya,G.A., Grollman,A.P. and Moriya,M. (2000) Mutagenesis induced by 1,N^6-ethenodeoxyadenosine adduct in human cells. *Cancer Res.*, **60**, 4098–4104.
15. Singer,B., Antoccia,A., Basu,A.K., Dosanjh,M.K., Fraenkel-Conrat,H., Gallagher,P.E., Kusmierek,J.T., Qui,Z.-H. and Rydberg,B. (1992) Purified human 1,N^6-ethenoadenine binding protein and 3-methyladenine-DNA glycosylase both act on 1,N^6-ethenoadenine and 3-methyladenine. *Proc. Natl Acad. Sci. USA*, **89**, 9386–9390.
16. Saparbaev,M., Kleibl,K. and Laval,J. (1995) *Escherichia coli*, *Saccharomyces cerevisiae*, rat and human 3-methyladenine DNA glycosylases repair 1,N^6-ethenoadenine when present in DNA. *Nucleic Acids Res.*, **23**, 3750–3755.

17. Gajewski,E., Rao,G., Nackerdien,Z. and Dizdaroglu,M. (1990) Modification of DNA bases in -mammalian chromatin by radiation-generated free radicals. *Biochemistry*, **29**, 7876–7882.
18. Dizdaroglu,M., Jaruga,P., Birincioglu,M. and Rodriguez,H. (2002) Free-radical-induced damage to DNA: mechanisms and measurements. *Free Radic. Biol. Med.*, **32**, 1102–1115.
19. Wood,M.L., Estave,A., Morningstar,M.L., Kuziamko,G. and Essigmann,J.M. (1993) Genetic effects of oxidative DNA damage: comparative mutagenesis of 7,8-dihydro-8-oxoguanine and 7,8-dihydro-8-oxoadenine in. *Escherichia coli. Nucleic Acids Res.*, **20**, 6023–6032.
20. Moriya,M. (1993) Single-stranded shuttle phagemid for mutagenesis studies in mammalian cells: 8-oxoguanine in DNA induces targeted G.C → T.A transversions in simian kidney cells. *Proc. Natl Acad. Sci. USA*, **90**, 1122–1126.
21. Tan,X., Grollman,A.P. and Shibutani,S. (1999) Comparison of the mutagenic properties of 8-oxo-7,8-dihydro-2′deoxyadenosine and 8-oxo-7,8-dihydro-2′-deoxyguanosine DNA lesions in mammalian cells. *Carcinogenesis*, **20**, 2287–2292.
22. Kamiya,H. (2003) Mutagenic potentials of damaged nucleic acids produced by reactive oxygen/nitrogen species: Approaches using synthetic oligonucleotides and nucleotides. *Nucleic Acids. Res.*, **31**, 517–531.
23. Kalam,M.A. and Basu,A.K. (2005) Mutagenesis of 8-oxoguanine adjacent to an abasic site in simian kidney cells: Tandem mutations and enhancement of G→T transversions. *Chem. Res. Toxicol.*, **18**, 1187–1192.
24. Kamiya,H., Murata-Kamiya,N., Koizume,S., Inoue,H., Nishimura,S. and Ohtsuka,E. (1995) 8-Hydroxyguanine (7,8-dihydro-8-oxoguanine) in hot spots of the c-Ha-ras gene. Effects of sequence contexts on mutation spectra. *Carcinogenesis*, **16**, 883–889.
25. Grollman,A.P. and Moriya,M. (1993) Mutagenesis by 8-oxoguanine: an enemy within. *Trends Genet*, **9**, 246–249.
26. Hazra,T., Izumi,T., Kow,Y.W. and Mitra,S. (2003) The discovery of a new family of mammalian enzymes for repair of oxidatively damaged DNA, and its physiological implications. *Carcinogenesis*, **24**, 155–157.
27. Parker,A.R. and Eshlemena,J.R. (2003) Human MutY: gene structure, protein functions and interactions, and role in carcinogenesis. *Cell. Mol. Life Sci.*, **60**, 2064–2083.
28. Al-Tassan,N., Chmiel,N.H., Maynard,J., Fleming,N., Livingston,A.L., Williams,G.T., Hodges,A.K., Davies,D.R., David,S.S., Sampson,J.R. *et al.* (2002) Inherited variants of *MYH* associated with somatic G:C-to-T:A mutations in colorectal tumors. *Nat. Genet.*, **30**, 227–232.
29. Haracska,L., Yu,S.-L., Johnson,R.E., Prakash,L. and Prakash,S. (2000) Efficient and accurate replication in the presence of 7,8-dihydro-8-oxoguanine by DNA polymerase η. *Nat. Genet.*, **25**, 458–461.
30. Basu,A.K., Niedernhofer,L.J. and Essigmann,J.M. (1987) Deoxyhexanucleotide containing a vinyl chloride-induced DNA lesion, 1,N^6-ethenoadenine: synthesis, physical characterization and incorporation into a duplex bacteriophage M13 genome as part of an *amber* codon,. *Biochemistry*, **26**, 5626–5635.
31. McGregor,W.G., Wei,D., Maher,V.M. and McCormick,J.J. (1999) Abnormal, error-prone bypass of photoproducts by Xeroderma pigmentosum variant cell extracts results in extreme strand bias for the kinds of mutations induced by UV light. *Mol. Cell. Biol.*, **19**, 147–154.
32. Nolan,S.J., McNulty,J.M., Krishnasamy,R., McGregor,W.G. and Basu,A.K. (1999) C8-guanine adduct-induced stabilization of a -1 frameshift intermediate in a nonrepetitive DNA sequence. *Biochemistry*, **38**, 14056–14062.
33. Li,J.J. and Kelly,T.J. (1985) Simian virus 40 DNA replication *in vitro*: specificity of initiation and evidence for bidirectional replication. *Mol. Cell Biol.*, **5**, 1238–1246.
34. Brewer,B.J. and Fangman,W.L. (1987) The localization of replication origins on ARS plasmids in S. cerevisiae. *Cell*, **51**, 463–471.
35. Hyrien,O. and Mechali,M. (1992) Plasmid replication in *Xenopus* eggs and egg extracts: a 2D gel electrophoretic analysis. *Nucleic Acids Res.*, **7**, 1463–1469.
36. Roberts,J.D. and Kunkel,T. A. (1988) Fidelity of a human DNA replication complex. *Proc. Natl Acad. Sci USA*, **85**, 7064–7068.
37. Little,R.D., Platt,T.H. and Schildkraut,C.L. (1993) Initiation and termination of DNA replication in human rRNA genes. *Mol. Cell. Biol.*, **13**, 6600–6613.
38. Dijkwe,P.A., Vaughn,J.P. and Hamlin,J.L. (1994) Replication initiation sites are distributed widely in the amplified CHO dihydrofolate reductase domain. *Nucleic Acids Res.*, **22**, 4989–4996.
39. Cordeiro-Stone,M., Liubov,S., Zaritskaya,L.S., Price,L.K. and Kaufmann,W.K. (1997) Replication fork bypass of a pyrimidine dimer blocking leading strand DNA synthesis. *J. Biol. Chem.*, **272**, 13945–13954.
40. Avkin,S., Adar,S., Blander,G. and Livneh,Z. (2002) Quantitative measurement of translesion replication in human cells: evidence for bypass of abasic sites by a replicative DNA polymerase. *Proc. Natl Acad. Sci. USA*, **99**, 3764–3769.
41. Fortini,P., Parlanti,E., Sidorkina,O.M., Laval,J. and Dogliotti,E. (1999) The type of DNA glycosylase determines the base excision repair pathway in mammalian cells. *J. Biol. Chem.*, **274**, 15230–15236.
42. Wyatt,M.D. and Samson,L.D. (2000) Influence of DNA structure on hypoxanthine and 1,N^6-ethenoadenine removal by murine 3-methyladenine DNA glycosylase. *Carcinogenesis*, **21**, 901–908.
43. Limoli,C.L, Giedzinski,E., Morgan,W.F. and Cleaver,J.E. (2000) Polymerase η deficiency in the xeroderma pigmentosum variant uncovers an overlap between the S phase checkpoint and double-strand break repair. *Proc. Natl Acad. Sci. USA*, **97**, 7939–7946.
44. Haracska,L., Prakash,S. and Prakash,L. (2003) Role of human DNA polymerase κ as an extender in translesion synthesis. *Mol. Cell. Biol.*, **23**, 1453–1459.
45. Haracska,L., Prakash,S. and Prakash,L. (2002) Yeast DNA polymerase ζ is an efficient extender of primer ends opposite from 7,8-dihydro-8-oxoguanine and O6-methylguanine. *Proc. Natl Acad. Sci. USA*, **99**, 16000–16005.
46. Haracska,L., Johnson,R.E., Unk,I., Phillips,B., Hurwitz,J., Prakash,L. and Prakash,S. (2001) Physical and functional interactions of human DNA polymerase η with PCNA. *Mol. Cell. Biol.*, **21**, 7199–7206.
47. Shiomi,Y., Masutani,C., Hanaoka,F., Kimura,H. and Tsurimoto,T. (2007) A second proliferating cell nuclear antigen loader complex, Ctf18-replication factor C, stimulates DNA polymerase η activity. *J. Biol. Chem.*, **282**, 20906–20914.
48. Dumstorf,C.A., Clark,A.B., Lin,Q., Kissling,G.E., Yuan,T., Kucherlapati,R., McGregor,W.G. and Kunkel,T.A. (2006) Participation of mouse DNA polymerase ι in strand-biased mutagenic bypass of UV photoproducts and suppression of skin cancer. *Proc. Natl. Acad Sci. USA*, **103**, 18083–18088.
49. Wang,Y., Woodgate,R., McManus,T.P., Mead,S., McCormick,J.J. and Maher,V.M. (2007) Evidence that in Xeroderma Pigmentosum variant cells, which lack DNA polymerase η, DNA polymerase ι causes the very high frequency and unique spectrum of UV-induced mutations. *Cancer Res.*, **67**, 3018–3026.
50. Pursell,Z.F., Isoz,I., Lundström,E.-B., Johansson,E. and Kunkel,T.A. (2007) Yeast DNA polymerase ε participates in leading-strand DNA replication. *Science*, **317**, 127–130.